

Rigid Paving Block Structures : Full Scale Experiments and Numerical Simulations

Herwig Hengl, Wolfgang Kluger-Eigl, Ronald Blab and Josef Füssl

Abstract

In recent years paving block structures with mortar filled vertical joint have become a favorite alternative to asphalt pavements, mainly in intra-urban regions. Whereas paving block structures with sand filled joint are used for areas with light or low trafficked roads, paving block structures with mortar filled joint may be used in all areas, even when heavy traffic loads are expected. Unfortunately, immature design concepts of such structures often lead to unexpected cracks resulting from thermal loadings. This motivated the construction of three large paving block test fields in Waldegg, Austria. A numerical simulation tool was developed and compared to data obtained from the test fields. By means of the simulation tool proposed in this chapter basic structural failure mechanisms for rigid paving blocks structures on splitbed could be obtained. Finally, estimates for necessary friction coefficients between paving blocks and splitbed to prevent large cracks are given.

1. Introduction and motivation

Paving block structures (pbs) have become a frequently used road construction method in urban areas. Thereby, increasingly applied is the construction of rigidly laid pbs, where the joints between paving blocks are filled with mortar. This rigidly laid pbs can be particularly beneficial when heavy traffic loadings are expected. Unfortunately, these structures often develop cracks on the surface, resulting from thermally induced stresses. These cracks affect the visual appearance but also the mechanical behaviour of these structures. As a consequence, the confidence and acceptance of this type of construction is reduced, which prevents it from a more frequent use.

As it comes to design codes for the construction of rigidly laid paving block structures, little information can be gained.In the German speaking region, rigid pbs are considered as a special construction method and only two guidelines offer recommendations for their planning and construction, namely: Forschungsgesellschaft für Straßen- und Verkehrswesen (2007) and Wissenschaftlich-Technische Arbeitsgemeinschaft für Bauwerkserhaltung und Denkmalpflege (2009). Both documents recommend the use of expansion joints and the latter mentions the positive influence of a strong adhesive bonding between the paving blocks and the mortar bed.

Nevertheless, extensive literature can be found regarding an equivalent problem: thermally induced stresses in concrete slabs and concrete pavements. Plannerer (1998), Rostasy and Kraus (2001), Röhling (2005), and Schikora and Eierle(1999) investigated thermal effects due to early stage hydration in concrete constructions. Bondy (1995), Schweighofer (2011), and Maliha (2005) engaged themself with thermal stresses and crack appearance in concrete pavements and slabs. Further contributions, Kolb (1988), Schütte (1997), and Petersson (1998) focuse on the interaction between concrete slabs and base layers. To the authors knowledge, only two works regarding numerical simulations of rigidly laid paving block structures, namely: Buchholz (2010) and Hengl et al. (2017b) can be found at the current moment. When it comes to numerical tools for paving block structures, several studies were published, which can be found in: Nishizawa et al. (1984), Jacobs and Houben (1988), Huurman et al. (1992), Lerch (2005), Ascher et al. (2006), Oeser and Chandra (2010), Füssl et al.

(2016b), and Hengl and Füssl (2016), to mention only a short selection of them.



Figure 1. Cracks resulting from thermally induced stress

The lack of reliable design concepts concerning rigidly laid pbs was the main motivation for this work. To gain better understanding of the mechanisms and causes in rigidly laid pbs that lead to crack occurance were the focus of this work. More specifically, the following questions arose and should be answered in this work:

1. Can the main results gained from full scale temperature loading tests be reproduced with numerical simulations?
2. When, where, and why are cracks occuring in such paving block structures?
3. What is the impact of the friction coefficient or bonding between paving blocks and the beneath layers on the mechanical performance of the paving block structure and how do these parameters affect the distance between cracks?
4. How does the fracture energy of interfaces between materials influence the occurrence of cracks in paving block structures?
5. To which extend are sublayers influencing the vertical load bearing capacity?
6. Based on a better understanding of rigid paving block structures, can any recommendations be given regarding the construction method?

To answer that questions, a full scale field experiment with three different pbs was carried out with industry partners in Waldegg, Austria. The details of the field experiments can be found in Section 2. In Section 3 the numerical model and the results of various numerical simulations are given. A final conclusion is given in Section 4.

2 Full scale field experiments

To evaluate the horizontal displacements of rigid paving block structures under real climatic conditions, three full scale test fields were constructed in November 2015.

2.1 Testfield layout

Usually guidelines recommend a maximum field length of 6 to 10 m for rigid pbs and the installation of expansion joints between the fields to compensate thermal expansion and contraction. To encourage the occurrence of cracks these guidelines were consciously ignored and the test fields were constructed without expansion joints and field lengths of 15 m.

Test fields

Three test fields were constructed at Waldegg, Austria in Winter 2015. These test fields were constructed over a length of 15 meters and with a width of 1 m each, separated by gravel-filled gaps of 20 cm. Horizontal movement was prevented by a rigid concrete bearing at the one end of the test fields. The opposite side of the pbs is not hindered in any way, allowing horizontal deformations to develop freely. The basic layout of the test field is shown in Figure 2.

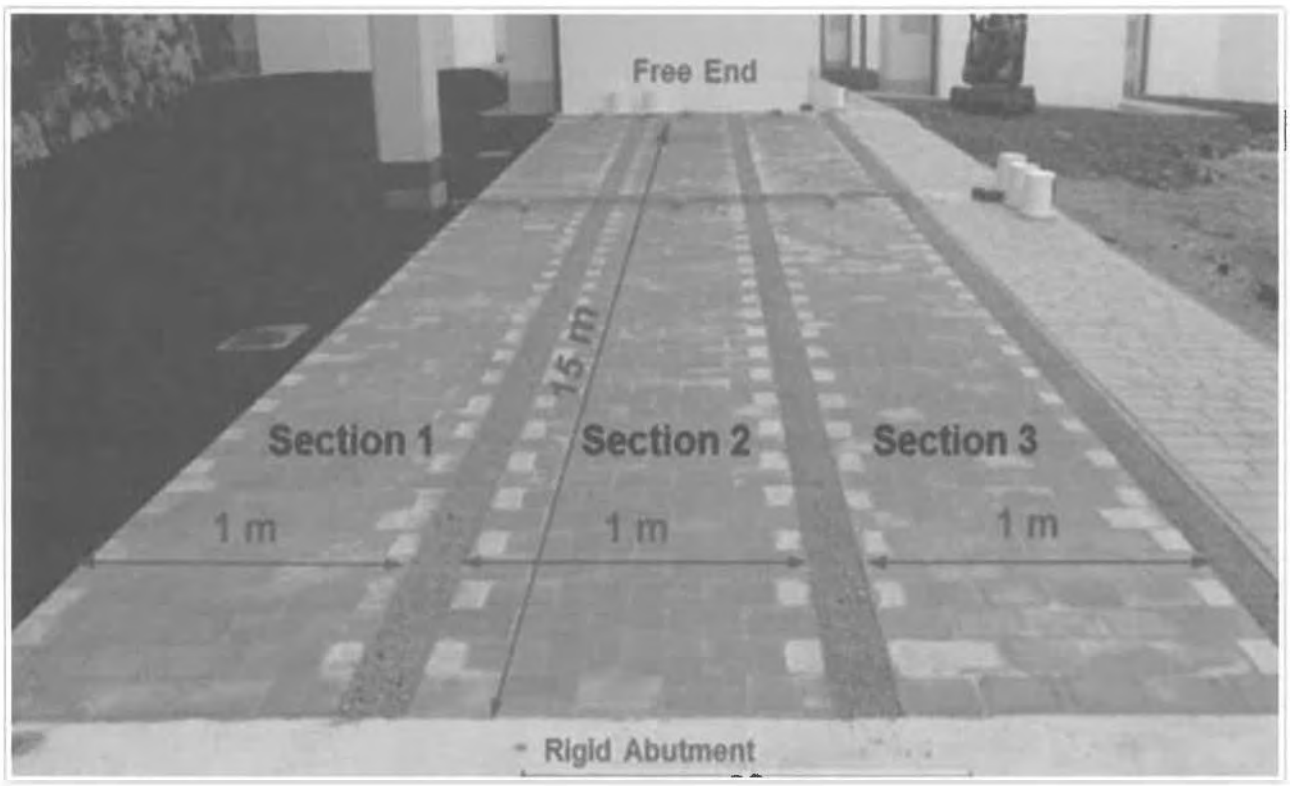

Figure 2. Basic layout of the three different paving block structures installed for full scale temperature experiments

Pavement Structures

The composition of the three different paving block pavements investigated is schematically illustrated in Figure 3. The test fields can be refereed to as:

- Test field 1: concrete blocks with mortar-filled joints laid in a mortarbed on a pervious concrete base course
- Test field 2: concrete blocks with mortar-filled joints laid in mortarbed on an unbound base course
- Test field 3: concrete blocks with mortar-filled joints laid in splitbed on an unbound base course

01_ Design and anlaysis of BP under heavy loading

Instrumentation

Six PT100 temperature sensors were built into test fields 1 and 2. They were placed on the surface, underneath the bedding (13 cm) and underneath the base course (-28 cm)to record the temperature in different depths of the pavement structure. Furthermore, six Wenglor CP35MHT80 laser distance sensors were appliedto the pavement surfaces to record horizontal deformations. They were placed in the middle and at the free end of each test field, as can be seen in Figure 4. In addition, a weather station was set up nearby to collect air temperature, rain, wind, and solar radiation.

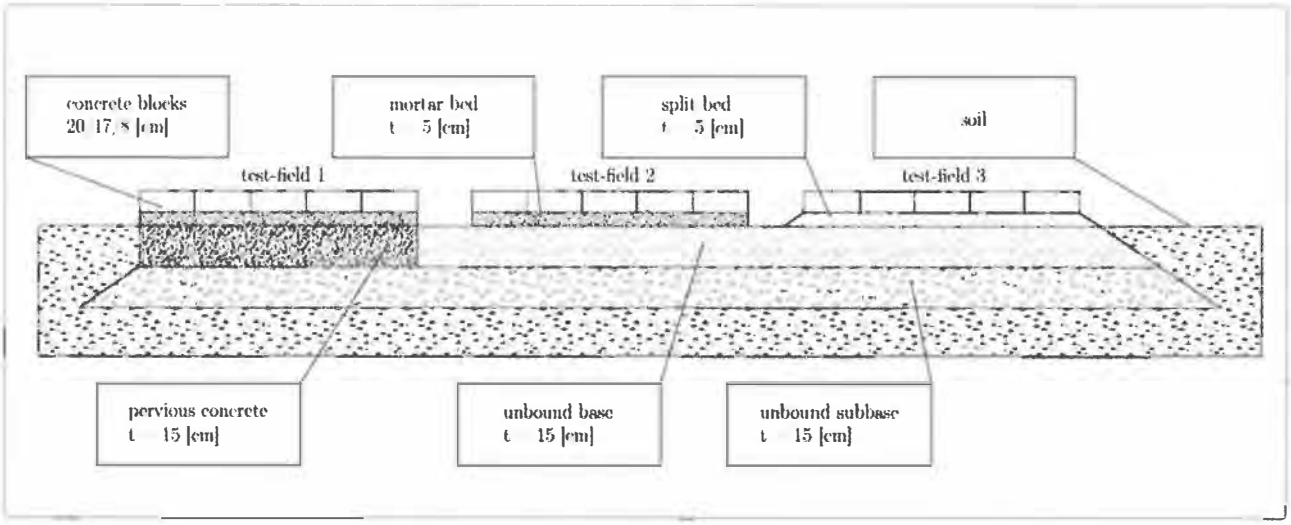

Figure 3. Three different paving block structures investigated in full scale field experiments

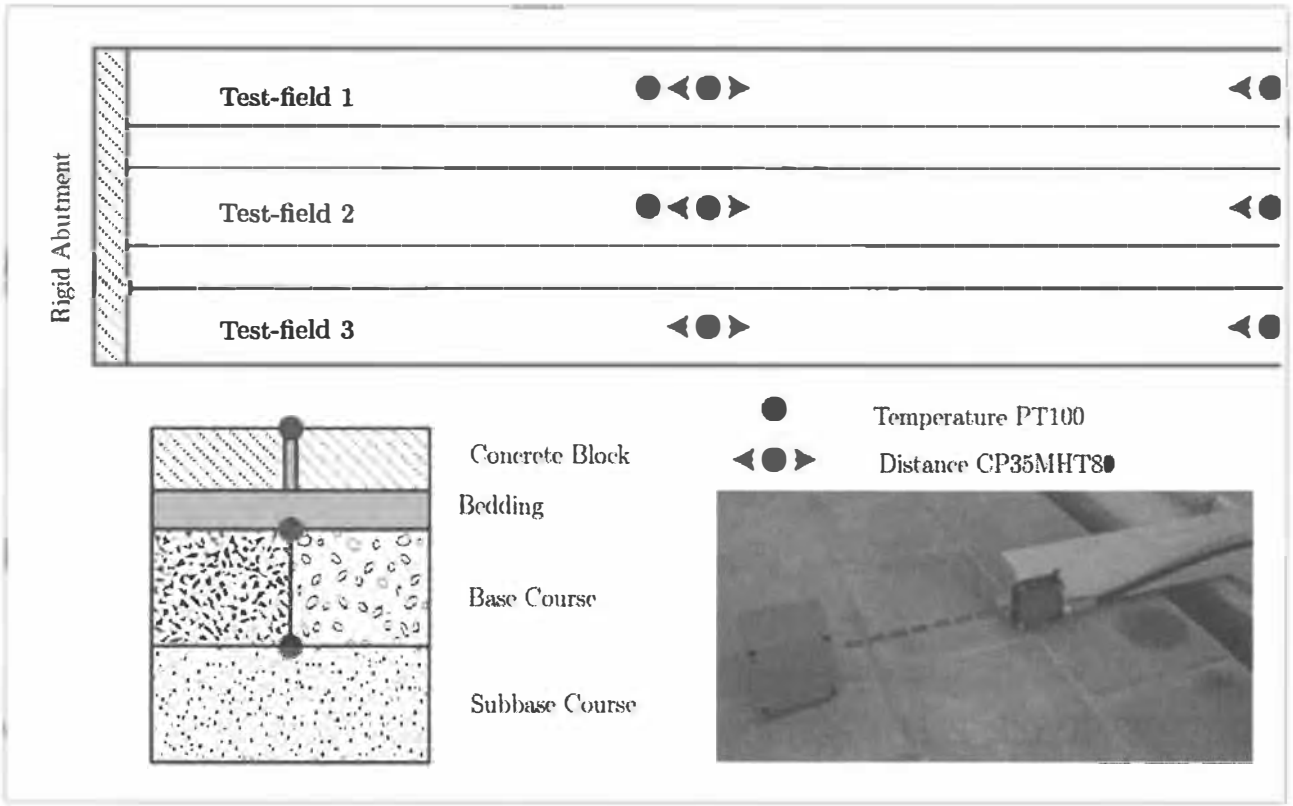

Figure 4. Instrumentation on Test Field

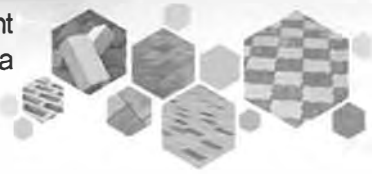

Construction

The test field was built in November and December 2015. After finishing the rigid concrete bearing, the anti-frost layer was constructed for all three test sections at once. On November 25th, 2015 at air temperatures of about 0°C, the base course for Section 2 and 3, and the pervious concrete base for Section 1 were constructed. On November 26th, 2015 the mortarbed for test field 1 was applied and the concrete paving blocks were laid into the bedding. The block pavement and the mortarbed of Section 2 were built on November 27th, 2015 and November 30th, 2015 at air temperatures between 3°C and 11°C. The concrete blocks of test field 3 were paved on splitbed afterwards. On Dezember 2nd, 2015 the joints of the three test fields were filled with cement mortar at air temperatures of about 10°C. Though the climatic conditions were not ideal for the construction of rigid pbs, the low construction temperatures were beneficial to obtain large deformations in summer.

2.2 Execution of full scale experiments

The experiments should deliver accurate temperatures in different layers of the pavement structures and correlated displacements due to the structures thermal expansion and contraction. The measurements were intended to be carried out for at least one year. Further, due to the design of the test fields, crack occurrence was expected and therefore visual inspections of the pavement surfaces were planned. The measurements can be listed as following:

- The temperature measurements, based on the temperature sensors built into test field 1 and 2, started on Dezember 25th, 2015 at an air temperature of 0°C. The measuring interval was set to 15 minutes.
- Horizontal deformation, which were measured in the middle and on the free end of the pavements surfaces, were obtained by laser distance sensors. This measurements also started on November 25th, 2015 and the measuring interval were set to 15 minutes.
- The aim of the visual inspection was to register surface damages, especially cracks. Therefore, inspections were planned after the first winter (May 2016), the first summer (October 2016), and in the second winter (December 2016). All damages were documented with videos and photos.

2.3 Results of full scale experiments

In a period of 13 months (till January 29th, 2017) over 260.000 temperature data points were recorded from sensors in the test fields and additional sensors which captured the air temperature. Temperature distributions of the air, on the pavements surface, beneath the bedding, and under the base course is shown in Figure 6 a. The minimum air temperature was −16,1◦C and the maximum +33,4◦C, leading to an air temperature range of approximately 50◦K. The maximum temperature difference on the pavements surfaces was 54◦K for the pavement surface, 39◦K underneath the bedding, and 30◦K underneath the base course. The results further reveal, thatthere were no major discrepancy of temperatures beneath the pervious concrete layer and beneath the unbound base layer. The temperatures beneath the bedding and the base courses followed the air temperature with a time delay of 1.5 to 6 hours, depending on the layers depth. The daily surface temperature courses of hot summer days reveal extreme temperature increases of 26◦K during 10 hours followed by a 14 hours decrease during the night. On cold winter days the pavements surface temperatures are generally higher than the air temperature and there are much less fluctuations (4◦K) during a 24 hour period than in summer. For longer cold periods of one week or more the temperatures in the bedding and the base course fell below 0◦C.

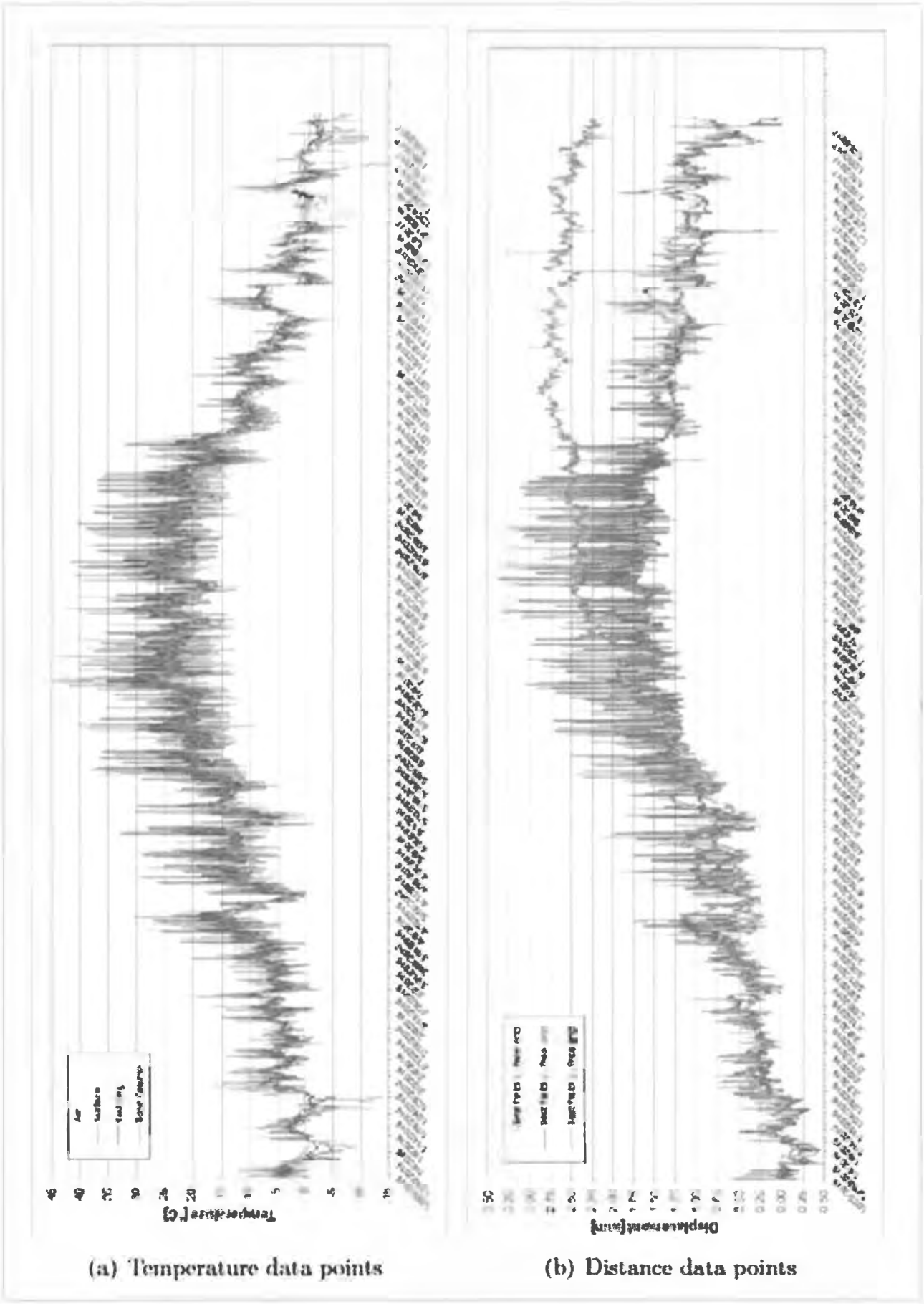

Figure 5. Results of temperature experiments



Deformation Analysis

In a period of 13 month (till January 29th, 2017) more then 220.000 distance data points were recorded from the distance sensors applied to the test fields surfaces. In Figure 6 b, the course of the horizontal deformation for the free end of the three test fields are presented. For each of the six sensors the minimum, the maximum, the mean, the range, and the standard deviation were calculated and are given summarised in Figure 1. The maximum compression of −0.6 mm was measured during the cold Period weeks in January 2016, where the temperatures were clearly below 0◦C. The maximum expansion of 3.4 mm was measured in the beginning of August 2016.

Period 25.12.2015-29.01.2017	Test-field 1		Test-field 2		Test-field 3	
Displacement [mm]	Middle	Free End	Middle	Free End	Middle	Free End
Minimum	-0.5	-0.5	-0.6	-0.5	-0.6	-0.2
Maximum	+0.5	+3.4	+0.9	+2.7	+0.8	+3.4
Range	1.0	3.9	1.4	3.2	1.4	3.6
Mean Value	0.0	1.2	0.0	1.0	0.1	1.6
Deviation	0.1	0.7	0.2	0.6	0.2	1.0

Table 1. Statistical analysis of Displacements for test sections 1, 2, and 3

The measurements show that the free end of the pbs can deform easily. In longitudinal direction the shear force increases, resulting from the interaction of the bound layer/layers to the unbound ones. As a consequence, the distance sensors in the middle of the structures only record measurements up to 0.9 mm, whereby at the free end of the structure almost 3.4 mm were recorded. Based on the experimental observations, the following statements can be made:

- The temperature gradient over the cross section of the construction causes incompatible deformations and is, thereby, holding back the deformation of structural elements with the highest temperature loads. This leads to temperature–induced internal stresses.
- The constant temperature part in the cross section drives the bound layers of the structure to contract/expand. As far as the bonding between these layers is intact, the deformation happens uniform to a great extend. Nevertheless, differences of thermal expansion coefficients may result in internal stresses and distortion of cross–sections.
- The deformations of the structure, resulting from the temperature gradient as well as from the constant part of the thermal loading, are restrained by the friction to the unbound layers. Usually the center of displacement lies in the center of mass. When the contraction is blocked, this center shifts. In case of the test fields, the center of displacements can be found at the rigid concrete bearing prior to any crack occurrence. The structure contractsuntil the (constant) thermally induced stress in the cross–section is equal to the summed up shear stresses occurring due to friction to the unbound bases. This effect can be examined by means of the numerical simulation results as shown in Figure 11 a. As can be seen, the deformations in the structures' half with the rigid bearing are almost completely blocked. This explains the low displacement measurements obtained by the sensors in mid field compared with the sensors at the free end, as illustrated in Figure 1. Figure 6 shows the interdependence of horizontal deformation and surface temperature for test field 1 and 3, respectively. The figure reveals the fact that the deformation of test field 1 (mortarbed on pervious concrete) are mainly reversible, while at test field 3 the cracks pervade the whole bound superstructure, leading to several independent parts of the structures with their own center of mass.

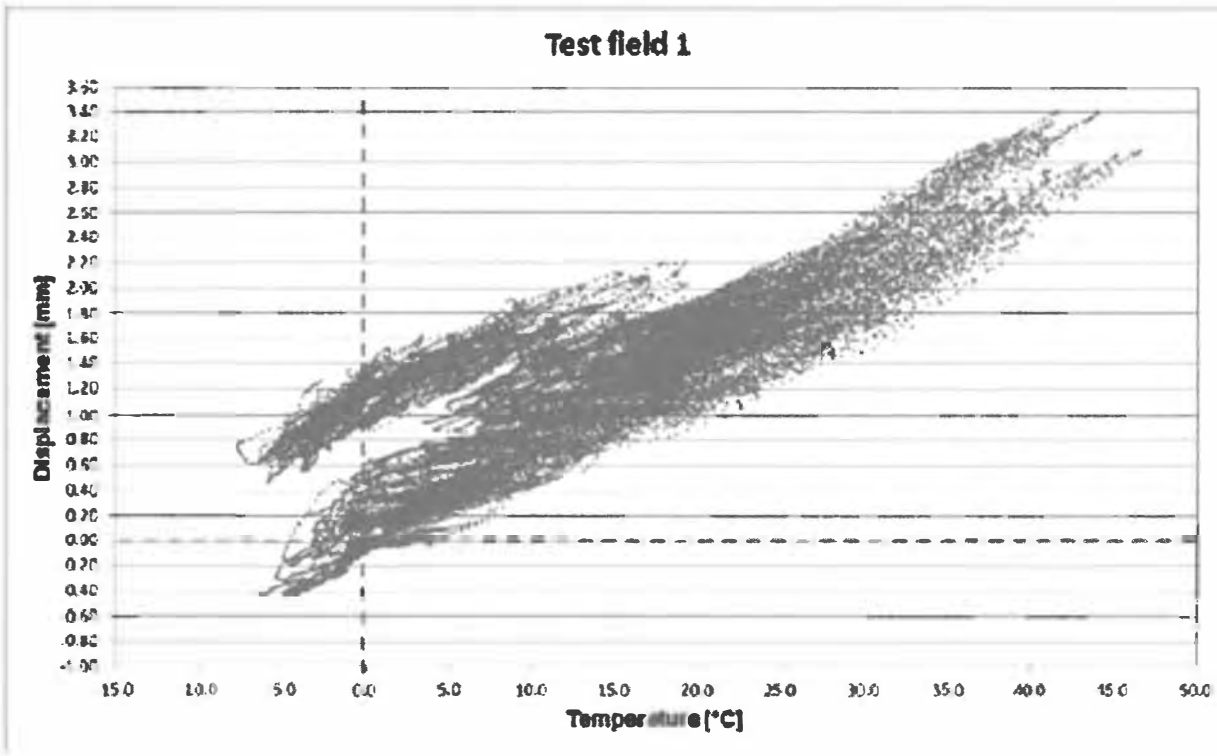

(a)

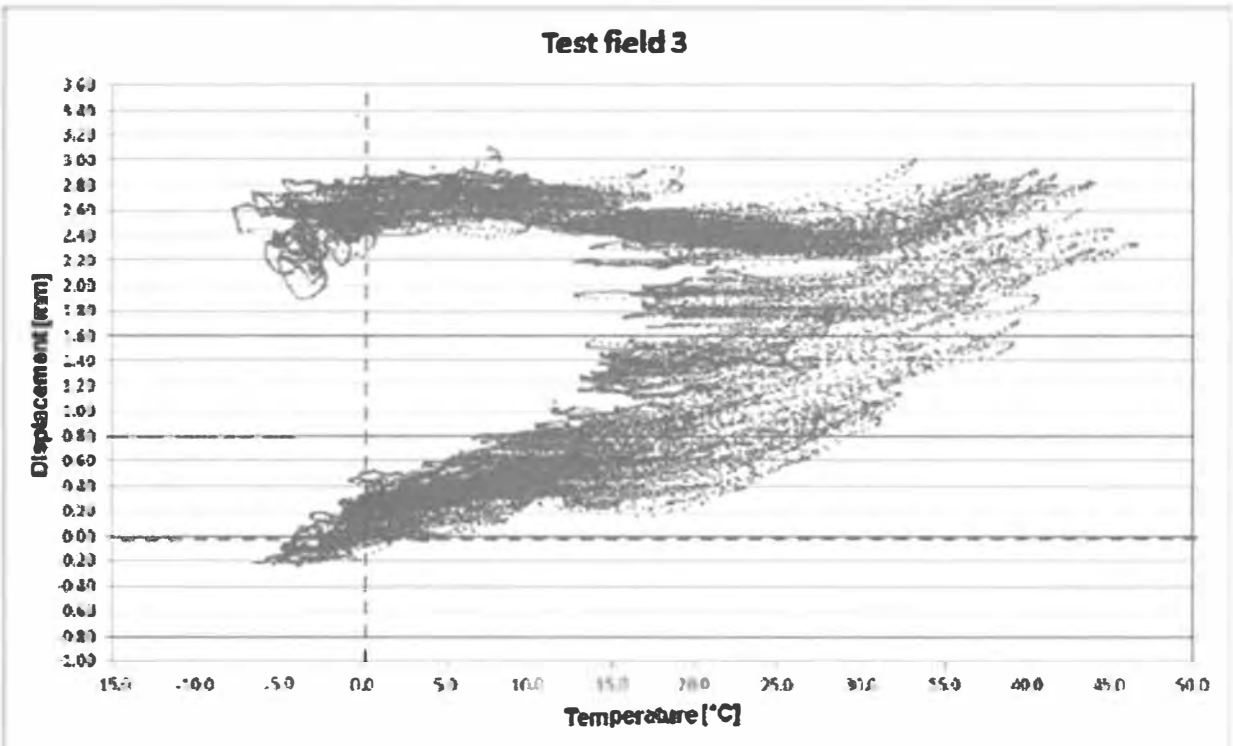

(b)

Figure 6. Interdependence of horizontal deformation and surface temperature for test field 1 and 3

Crack Distribution

The first visual inspection of the test fields were carried out in May 2016. No damage or cracks appeared in test sections 1 and 2. Nevertheless, on test field 3 three very fine cracks were found. Those cracks were about 5 m apart, so the spacing was approximately a third of the length of the test section. After summer the visual inspection in October 2016 showed also some fine cracks in test sections 1 and 2, approximately in the middle and a quarter of the section length. In test section 3 the cracks increased and the spacing was approximately an eight of the length. Two cracks in the last third (row 58 and 73) were nearly 1 mm wide (Figure 7 b). During inspections in December 2016, three additional fine cracks were found in the lastthird of test field 1. On test field 2 two additional fine cracks were identified and the largest crack opened up to 1mm. Test field 3 was nearly unchanged compared to the last inspection. An overview of the cracks on test fields surfaces in May, October, and December 2016 is given in Figure 6.

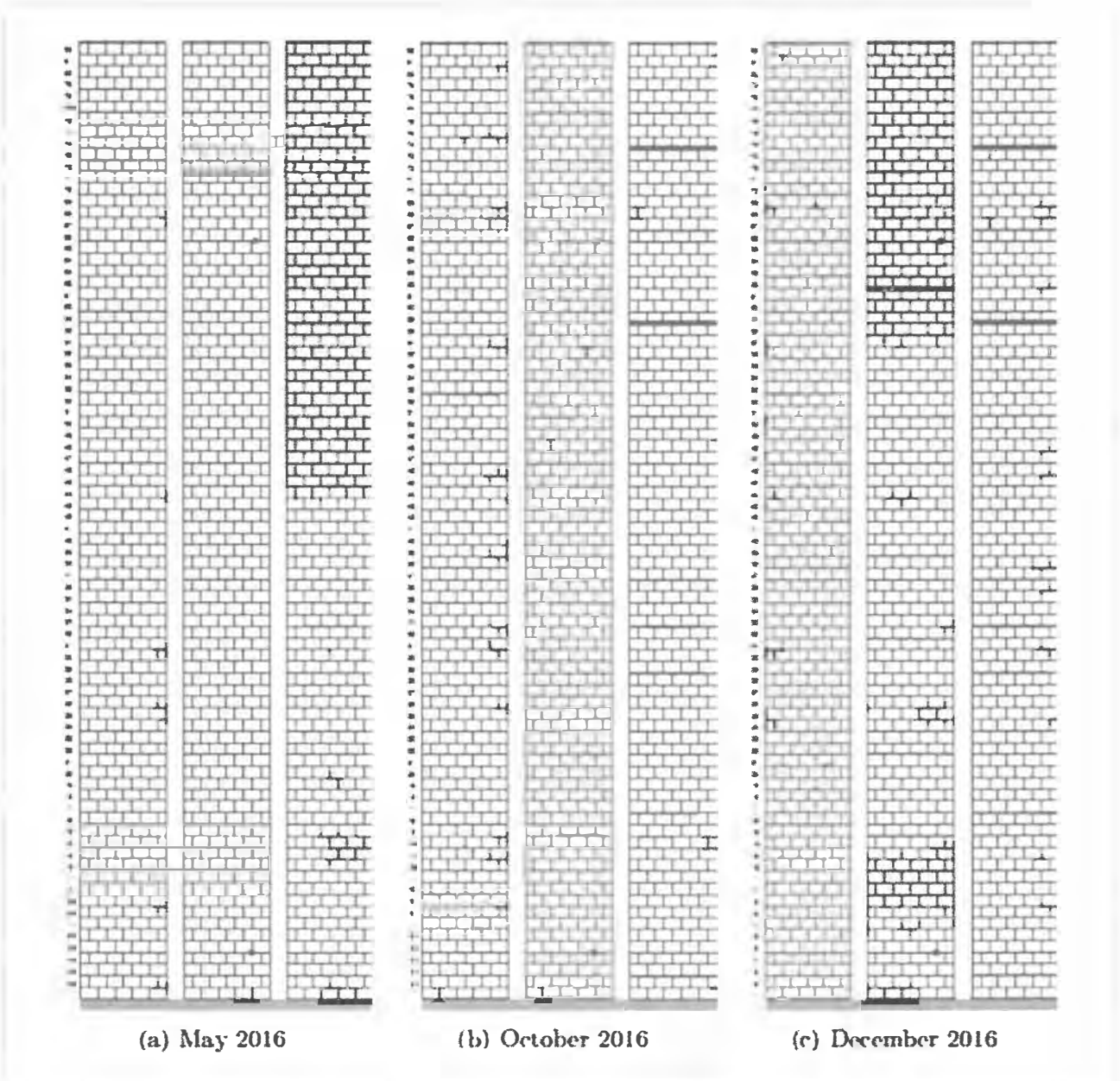

Figure 7. Overview of crack patterns on the three test fields, recorded at three different times.

The normal stress is respectively constant for that part of the superstructure. The occurrence of the first crack can happen at any joint in this region, but usually occurs close to the rigid bearing due to the increased local stiffness. After this first cracks appears, the stress is decreasing with increasing crack width, as defined by the linear cohesive damage evolution law, which is determined by 0.001 mJ/mm^2 . The center of the contraction shifts towards the middle as the contact interaction gets weaker with the increasing thermal load.

In the illustrated displacement field in Figure 6 a, the remaining temperature is not sufficient to open up the crack further then 0.22 mm. When the friction coefficient increases the crack opens up at a lower thermal loading, leaving more thermal contraction for the increase of the crack widths. Due to the opening of the crack, friction occurs, and the normal stresses in the superstructure increase until the next crack opens, as illustrated in Figure 11 a to d.

Another significant parameter is the fracture energy. Figure 14 shows the variation of the fraction energy from 0.00001 to 10 [mJ/mm^2] with a steady friction coefficient between paving blocks and splitbed. The number of cracks is highly dependent on the fraction energy.For high values of fracture energy the cracks cannot open and stress is still transmitted between blocks. For reduces values of fracture energy of about 0.25 [mJ/mm^2], the first crack can open up and the crack opening is quite high. When the fracture energy is further reduced more and more cracks open up. But the crack opening diminishes as the contraction is divided into several cracks.

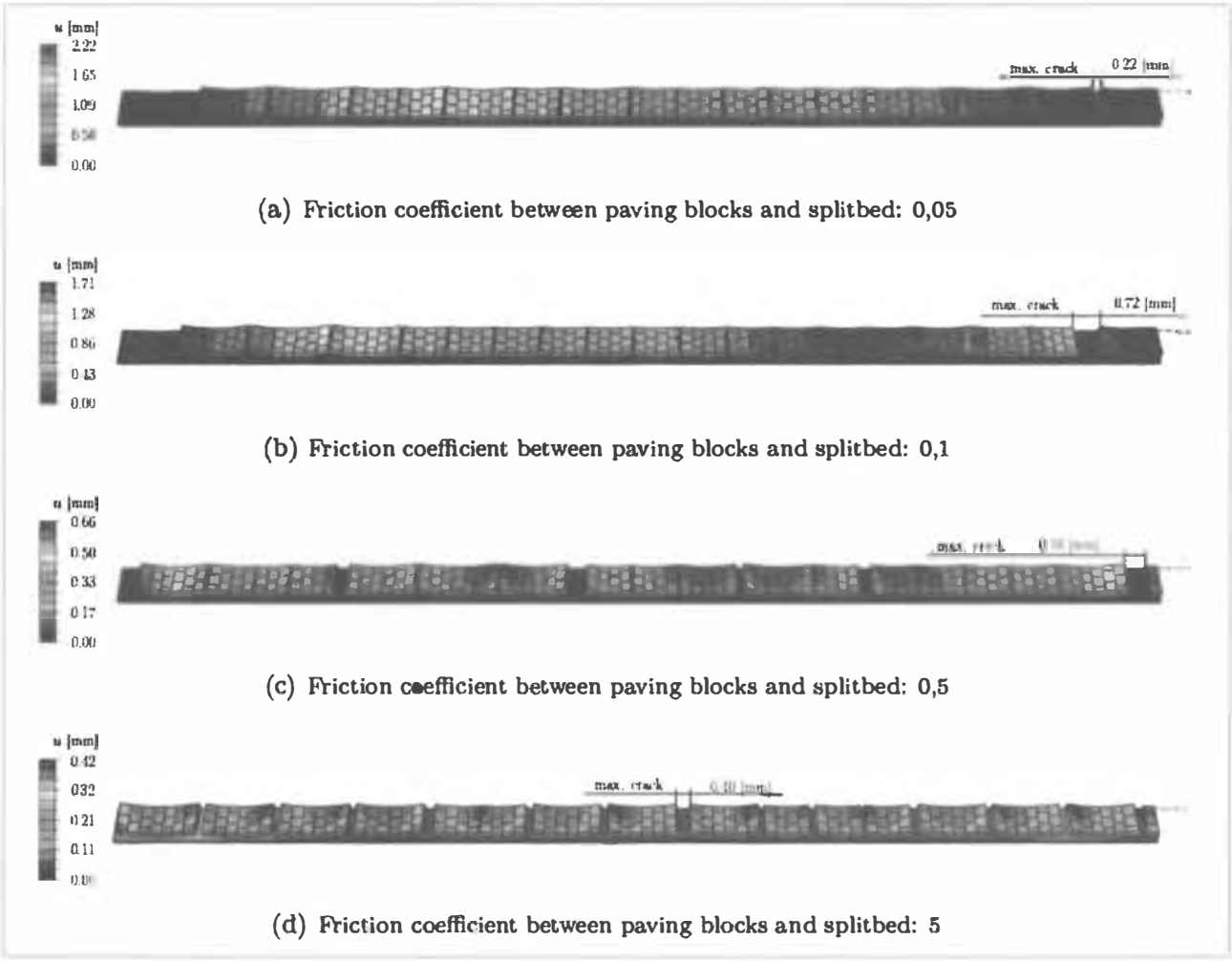

Figure 12. Resulting displacement fields obtained from simulations of test field 3

3.3 Results of FWD simulations

To get to a good correlation with the field experiments the E-modulus of the soil had to be increased to 490 MPa. It is assumed that this high stiffness results from a strong compression and/or from consolidation due to neighboring buildings. The numerical results show a good correlation with the mean values obtained by the FWD experiments for each test field. Figure 16 illustrates the results from the FWD simulations of the test fields compared with the average values from the FWD measurements. It can be seen that the maximum deformation agrees very well, whereby the course of the vertical deformation in distance with the load center varies significantly. It is assumed that a to high stiffness for the loaded steelplate is the reason for that effect. Nevertheless, the deformation field of test field 3 can be found in Figure 15. The distribution of vertical deformation along the bound superstructure can be seen. Whereas in the perpendicular direction a strong deformation over the cross-section is found. A modification of the model under usage of symmetry boundary conditions will be used for a further comprehensive parameter study.

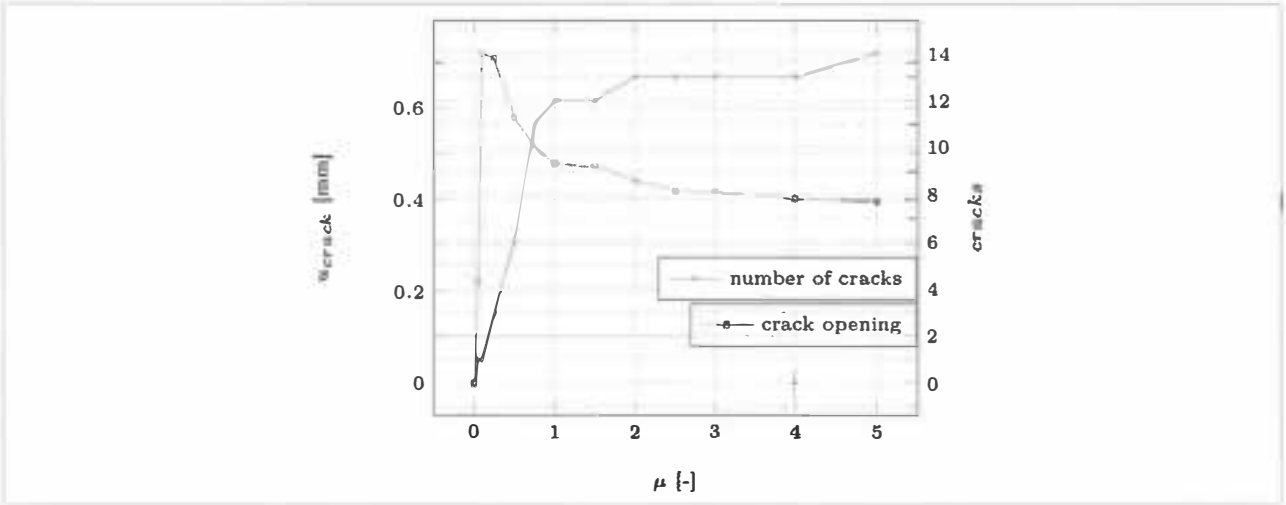

Figure 13. Maximum crack opening and number of appearing cracks for different friction coefficients between paving blocks and splitbed (test field 3).

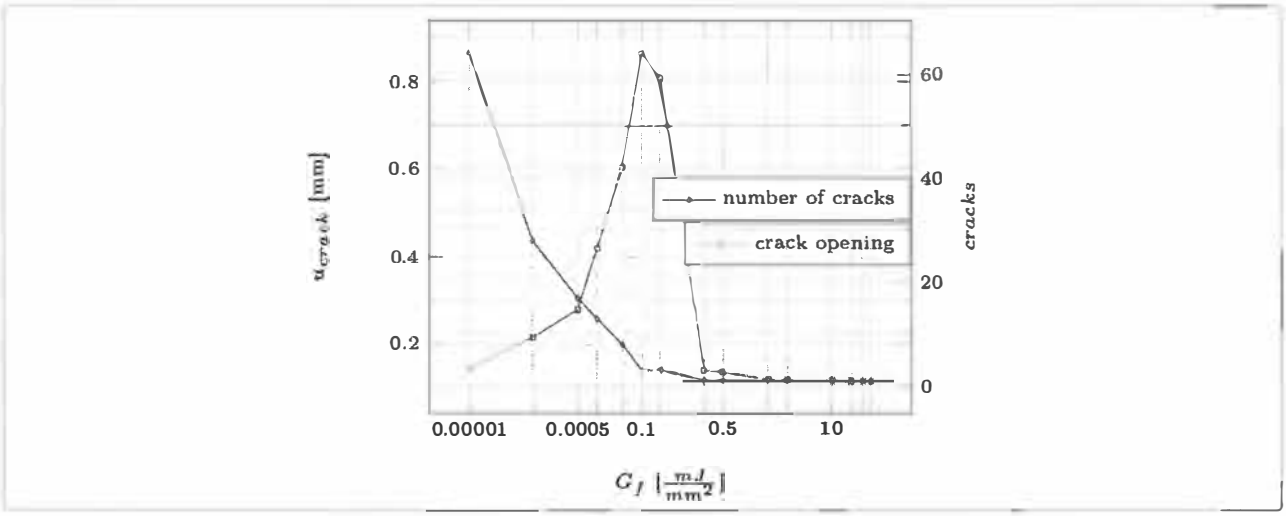

Figure 14. Maximum crack opening and number of cracks for different fracture energies of vertical joints (test field 3).

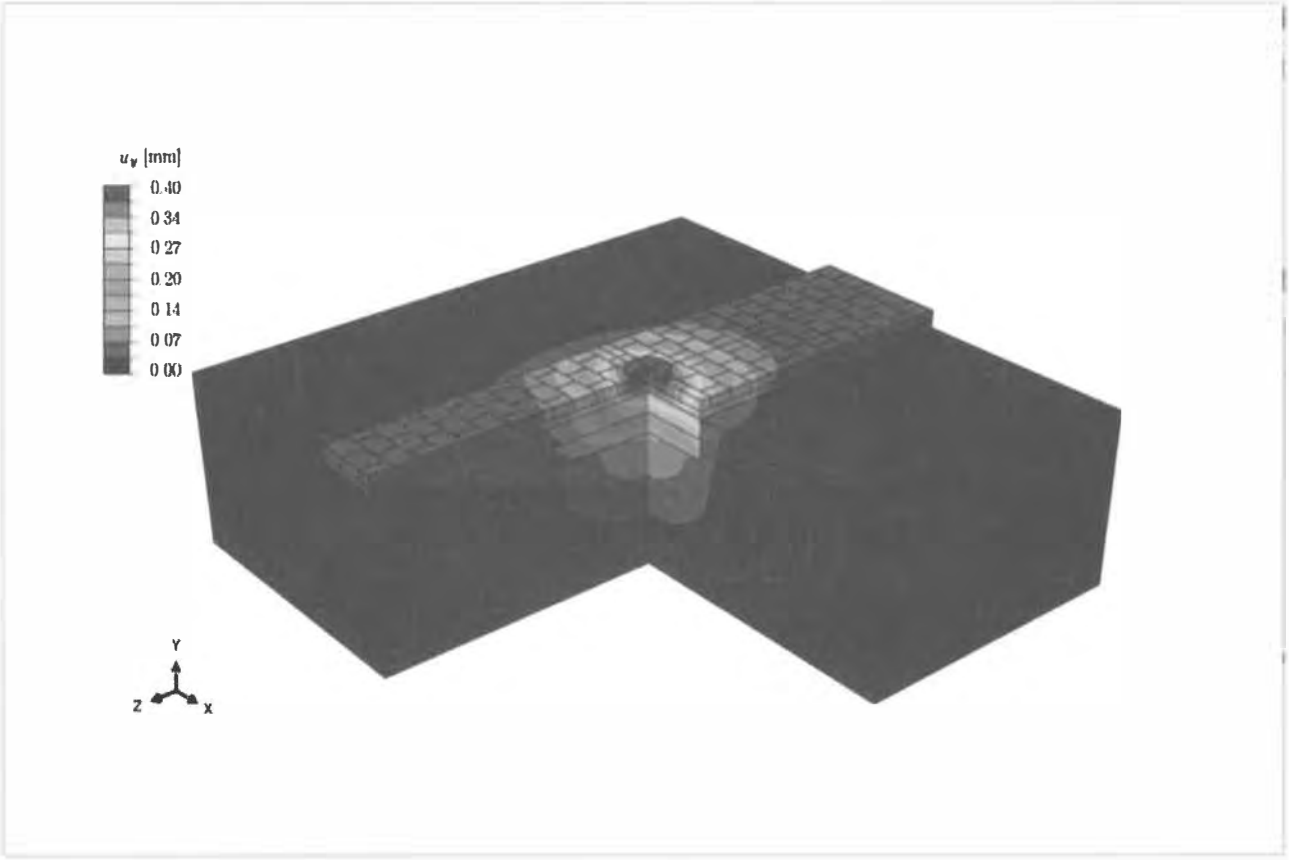

Figure 15. Vertical displacement field obtained from vertical loading simulations on test field 3.

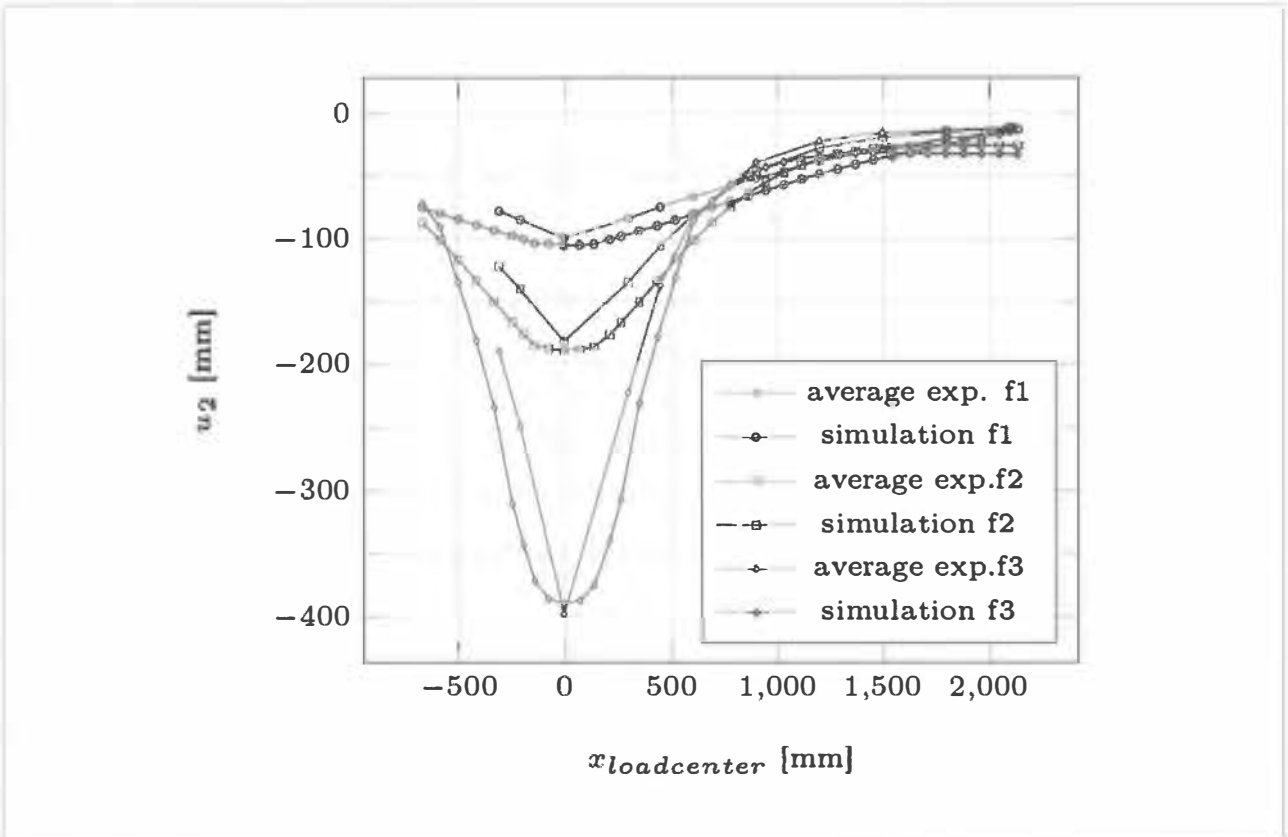

Figure 16. Results of falling-weight-deflector experiments compared to the corresponding numerical results.

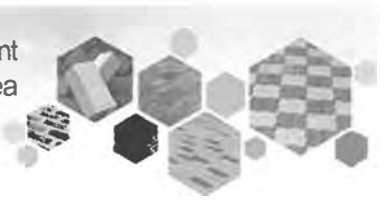

4. Conclusion

The full scale field experiment made it possible to achieve important knowledge regarding temperature, displacement, and crack behaviour of paving block structures with mortar-filled joints. Visual inspections revealed a significant difference regarding the number and width of cracks on the three test fields. On test field 1 (mortar bed on drainage concrete) far less cracks formed than on test field 2 (mortarbed on unbound base course). On test-field 3 (splitbed on unbound base course) two significant cracks with a width of 1 mm developed. These cracks occurred during the summer period 2016 and increased in width until winter 2016. Additional measurements with a falling weight deflectometer (FWD) revealed the differences of the load bearing capacities of the investigated testfields. Realistic temperature gradients were obtained and could be implemented into numerical models.

The results obtained from the test fields could be reconstructed by means of numerical simulation after adjusting the friction coefficient between paving blocks and splitbed, the fracture energy, and damage initiation values for the cohesive surface-to-surface interaction of the vertical joints between paving blocks. To reproduce the FWD results, the stiffness of the soil layer had to be increased. For the half of the test fields with the rigid concrete bearing, displacements of approximately 1 mm were measured.

The distance sensors on the free end of the test fields measured displacements of 3 mm to 4 mm. These results correlate with insights obtained by numerical simulations. The conclusions of this work can be summarized as follows:

- Normal stresses, leading to cracks on the surface of paving block structures with mortar-filled joints, result due to thermal loading either from the thermal gradient, from varying thermal expansion ratios within the bounded layers, or due to hampered or restricted contraction of the structure occurring from friction to the unbound sublayer. The stresses resulting from friction to the unbound sublayer are accumulated, beginning from the free end of the test field, until either: (1) the cohesive strength of the mortar bed is reached and cracks opening up, which decreases the internal stress, or (2) an equilibrium between the internal stresses in a cross-section of the structure and accumulated shear forces is found, subsequently, the structure stops contracting and no more frictional shearstresses occur, or (3) the whole contact area between paving blocks and splitbed exceeds the sticking friction and thereby contracts.
- The fiction coefficient between paving blocks and splitbed indeed seems to have a very large impact on the performance of a paving block superstructure under temperature loading. A characteristic friction coefficient lower than 0.8 MPa avoids the occurrence of distinct large cracks according to the performed numerical investigation, for the specific length of the test field. In case of longer paving block structures with mortar-filled joints, this value will decrease. Friction coefficient values around 0.6 MPa are usually found in literature for friction coefficients between concrete and unbound layers. It can be assumed that the experimentally-obtained friction coefficient values are exceeded in reality, resulting from intrusion of joint mortar into the splitbed, from unevenness of the splitbed, or other blockings of paving block displacements.

To obtain further insights, the extraction of drilling cores is planned. The pass through of cracks on test field 2 could explain the divergence of the crack occurrence between test field 2 and 3. For a further usage of the test fields, different methods for crack repair and their influence on load distribution and durability will be examined.

References

[1] Nishizawa, T., Matsuno, S., and Komura, M. (1984). Analysis of interlocking block pavements by finite element method. International Conference on Concrete Block Paving, Kanazawa University.

[2] Kolb, H. (1988). Ermittlung der Sohlreibung von Gründungskörpern unter horizontalem klimatischen Zwang. PhD thesis, TH Stuttgart.

[3] Jacobs, M. and Houben, L. (1988). Wheel testing and finite element analysis of concrete block pavement. Delft University of Technology.

[4] Huurman, M., Houben, L., and Kok., A. (1992). Development of a three-dimensional finite element model for concrete block pavements. Proceedings Fourth International Conference on Concrete Block Paving, Delft University of Technology.

[5] Bondy, K. (1995). Cracking in ground-supported post-tensioned slabs on expansive soil, pti technical notes, Canoga Park, California.

[6] Schütte, J. (1997). Einfluss der Lagerbedingungen auf Zwang in Betonbodenplatten. PhD thesis, TU Braunschweig.

[7] Plannerer, M. (1998). Temperaturspannungen in Betonbauteilen während der Erhärtung. PhD thesis, Technische Universität München.

[8] Petersson, D. (1998). Stresses in concrete structures from ground restraint. PhD thesis, Lund Inst. of Technology.

[9] Schikora, K. and Eierle, B. (1999). Berechnungsmodelle für Betonbauteile unter frühem Temperaturzwang. Tagungsband Baustatik-Baupraxis 7, Balkema-Verlag, TU München.

[10] Rostasy, F. and Kraus, M. (2001). Frühe Risse in massigen Betonbauteilen - Ingenieurmodelle für die Planung von Gegenmaßnahmen. Deutscher Ausschuss für Stahlbeton, TU Braunschweig.

[11] Röhling, S. (2005). Zwangsspannungen infolge Hydratationswärme. Verlag Bau+Technik.

[12] Maliha, R. (2005). Untersuchungen zu wirklichkeitsnahen Beanspruchungen in Fahrbahndecken aus Beton. PhD thesis, Universität Fridericiana zu Karlsruhe.

[13] Lerch, T. (2005). Investigation of the deformation behaviour of concrete block pavements under simulated traffic loading. PhD thesis, TU Dresden.

[14] Ascher, D., Lerch, T., Oeser, M., and Wellner, F. (2006). 3D-FEM Simulation of concrete block pavement. The 8th international conference on concrete block paving sustainable paving for our future, Interlocking Concrete Pavement Institute (ICPI), San Francisco.

[15] Forschungsgesellschaft für Straßen- und Verkehrswesen (2007). Arbeitspapier: Flächenbefestigungnen mit Pflasterdecken und Plattenbelägen in gebundener Ausführung, Vienna.

[16] Wissenschaftlich-Technische Arbeitsgemeinschaft für Bauwerkserhaltung und Denk-malpflege (2009). Merkblatt: Gebundene Bauweise Historisches Pflaster.

[17] Oeser, M. and Chandra, H. (2010). Segmented concrete block pavements: Analysis with optimized numerical tool. Betonwerk und Fertigteil-Technik 76.1, The University of New South Wales.

[18] Buchholz, J. (2010). Gebundene Pflasterbauweisen. PhD thesis, Universität Kassel.

[19] Schweighofer, A. (2011). Zwangsspannungen im jungen Beton in Bodenplatten und Wänden. PhD thesis, TU Vienna.



[20] Füssl, J., Kluger-Eigl, W., and Blab, R. (2016). Experimental identification and mechanical interpretationof the interaction behavior between concrete paving blocks. International journal of pavement engineering, Vol. 17, Pages 478-488, doi: 10.1080/10298436.2014.993205, TU Wien.

[21] Hengl, H. and Füssl, J. (2016). The influence of superelevated profiles of paving block structures on their load-bearing behavior. Engineering Structures, Vol 117, Pages 195-203, doi: 10.1016/j.engstruct.2016.03.003, TU Wien.

[22] Hengl, H., Kluger-Eigl, W., Blab, R., and Füssl, J. (2017). The performance of paving block structures with mortar filled joints under temperature loading, accessed by means of numerical simulations. Road Materials and Pavement Design, Pages 1-20, doi: 10.1080/14680629.2017.1330221, TU Wien.